Receding Horizon Voltage Control in LV Networks with Energy Storage

Donato Zarrilli†, Antonio Giannitrapani, Simone Paoletti, Antonio Vicino

Abstract— **The ever-growing penetration of low carbon technologies is causing important modifications of standard power flow patterns in electricity distribution grids. As a consequence, low voltage networks are frequently experiencing over- and undervoltages, resulting in a poor voltage quality at customers' premises. In this context, energy storage is deemed a key technology to meet power quality requirements. In this paper, a voltage control algorithm based on a receding horizon scheme is developed to operate the energy storage systems deployed in a low voltage network. The proposed procedure requires few measurements to forecast the future state of the network and anticipate possible voltage problems. The algorithm is applied to real data from an Italian low voltage network, consisting of demand and generation profiles which determine over- and undervoltages in the absence of voltage control. The obtained results highlight the potential of the proposed approach to reduce the amount of voltage violations over time.**

I. Introduction

Over- and undervoltages are becoming frequent in low voltage (LV) networks due to the growing penetration of low carbon technologies such as distributed generation (DG), electric vehicles and heat pumps. These are indeed causing significant modifications of typical power flows, resulting in a degradation of the quality of supply at consumers' premises. Therefore, maintaining voltage between specified limits has become one of the main issues currently faced by distribution system operators (DSOs). A radical solution consists of replacing existing cables and/or transformers with new equipments. The use of on-load tap changers (OLTC) at secondary substations to cope with voltage rise caused by increasing penetration of photovoltaic (PV) systems is proposed in [1]. In [2], different voltage control schemes involving active and reactive power control of DG inverters are compared. However, depending on technical, economic and/or regulatory issues, these solutions may not be implementable in practice. In this context, an alternative which is receiving increasing attention is represented by energy storage systems (ESSs), see, e.g., [3]-[6] and references therein. Pros of the use of ESSs are that voltage problems are solved locally, thus limiting the impact on the medium voltage (MV) network, and no curtailment of renewable generation is required.

Irrespective of the solution adopted, most of the approaches proposed in the literature address voltage support without any prediction of the future state of the network. This is mainly due to the poor availability of measurements in LV networks, making state reconstruction and forecasting a challenging problem. Since a full information, centralized approach would require complete monitoring of the network, some authors have studied different partial information setups to make voltage control both viable and reliable. In [7] the performance of an OLTC control logic is assessed under three different remote monitoring schemes, namely measurements taken at the middle, end, or middle and end of each feeder. The coordinated control scheme in [3] exploits a centralized controller, deciding which ESSs are to be activated upon the occurrence of a voltage problem, and dedicated decentralized controllers, one for each ESS, having visibility only of local voltage measurements. However, when ESSs are used, lack of predictive capability may turn out into sending the control signals with delay and without the guarantee that ESSs are ready for the required actions (e.g., battery levels are low when power supply to the network is required).

The approach taken in this paper is to use forecasts of demand and generation to "anticipate" the occurrence of voltage issues, and counteract them in advance. To this aim, predicted demand and generation are exploited in a suitable multi-period optimal power flow (OPF) problem with voltage constraints, whose solution returns the control policy for each ESS over the considered prediction horizon. In order to cope with uncertainties such as inaccurate forecasts, a receding horizon scheme is applied. At each time step, the multi-period OPF is solved over the whole prediction horizon, but only the control inputs for the first time step are applied. ESS control based on a receding horizon scheme is considered in [8], [9] for grid-connected microgrids. Differences with respect to our work mainly consist in the adopted network model and the formulated optimization problem. In our approach, simple predictive models are built to forecast demand and generation at each bus of the network. To this aim, only the power exchanged with the MV network and some meteorological variables (e.g., outdoor temperature and solar irradiance) are assumed to be measured in real-time at the MV/LV substation.

The paper is organized as follows. Section II presents the network model and the formulation of the optimal ESS operation problem, whose receding horizon implementation is then described in Section III. Load and generation forecasting is addressed in Section IV. Section V reports simulated results on a real Italian LV network, and conclusions are drawn in Section VI.

II. Problem formulation

In this section, we first describe the power flow model of a LV network equipped with ESSs. Then, we introduce

The authors are with the Dipartimento di Ingegneria dell'Informazione e Scienze Matematiche, Università di Siena, Siena, Italy.

† Corresponding author (zarrilli@dii.unisi.it).

an OPF problem for optimal operation of these ESSs. In the following, for a fixed sampling time ΔT, the value of a variable x at time $t\Delta T$ is denoted by $x(t)$, where $t = 0, 1, \dots$ is the discrete time index. The h-step ahead prediction of the variable x, based on the information available at time t, is denoted by $\hat{x}(t+h|t)$, with h being a positive integer. Moreover, the real part, imaginary part and complex conjugate of $z \in \mathbb{C}$ are denoted by $\mathrm{Re}(z)$, $\mathrm{Im}(z)$ and z^*, respectively.

A. Network model

Consider a LV network described by a graph $(\mathcal{N}, \mathcal{E})$, where $\mathcal{N} = \{1, 2, \dots, n\}$ is the set of nodes (*buses*) and $\mathcal{E}$ is the set of edges (*lines*). The admittance-to-ground at bus i is denoted by y_{ii}, while $y_{ij} = y_{ji}$ denotes the line admittance between nodes i and j. If $(i,j) \notin \mathcal{E}$, $y_{ij} = 0$. The network admittance matrix $Y = [Y_{ij}] \in \mathbb{C}^{n \times n}$ is a symmetric matrix defined as

$$Y_{ij} = \begin{cases} y_{ii} + \sum_{h \neq i} y_{ih} & \text{if } i = j \\ -y_{ij} & \text{otherwise.} \end{cases} \tag{1}$$

Let $V_k(t)$, $P_k(t)$ and $Q_k(t)$ denote the complex voltage, active power injection and reactive power injection at bus k and time t, respectively. These quantities are linked by the power balance equations

$$P_k(t) = \mathrm{Re}\left(V_k(t) \sum_{j \in \mathcal{N}} V_j^*(t) Y_{kj}^*\right) \tag{2a}$$

$$Q_k(t) = \mathrm{Im}\left(V_k(t) \sum_{j \in \mathcal{N}} V_j^*(t) Y_{kj}^*\right). \tag{2b}$$

Bus 1 is assumed to be a slack bus, characterized by fixed voltage magnitude and phase, i.e. $V_1(t)$ is known for all t. Conversely, complex voltages $V_k(t)$ at buses $k \in \mathcal{N}^L = \{2, \dots, n\}$ are determined by the power flow equations. For them, voltage quality requirements impose the magnitude to remain within specified limits, i.e.

$$\underline{v}_k^2 \leq |V_k(t)|^2 \leq \overline{v}_k^2, \tag{3}$$

where $\underline{v}_k \leq \overline{v}_k$ are given bounds. The real power flow from bus i to bus j can be also bounded to reflect the physical properties of the lines. This implies the constraint

$$\mathrm{Re}\left(V_i(t)\big[V_i(t) - V_j(t)\big]^* y_{ij}^*\right) \leq \overline{P}_{ij}, \tag{4}$$

whose left-hand side is the real power transferred from bus i to bus j at time t, and $\overline{P}_{ij} = \overline{P}_{ji}$ is a given upper bound.

Let $\mathcal{S} \subseteq \mathcal{N}^L$ be the set of buses equipped with ESSs. For $s \in \mathcal{S}$, $e_s(t)$ denotes the storage level at bus s and time t. Moreover, $r_s(t-1)$ and $b_s(t-1)$ are the average active and reactive power exchanged by the ESS between $t-1$ and t. The dynamics of $e_s(t)$ are modelled by the first-order difference equation $e_s(t) = e_s(t-1) + r_s(t-1)\Delta T$, whose solution is given by

$$e_s(t) = e_s(t_0) + \sum_{\tau=t_0}^{t-1} r_s(\tau) \Delta T, \tag{5}$$

with $e_s(t_0)$ being the initial storage level, which is assumed to be known. The storage level $e_s(t)$ is bounded as follows

$$0 \leq e_s(t) \leq E_s, \tag{6}$$

with E_s being the storage capacity installed at bus s. Both $r_s(t-1)$ and $b_s(t-1)$ are also bounded to reflect the ESS technology adopted, namely

$$\underline{R}_s \leq r_s(t-1) \leq \overline{R}_s \tag{7a}$$

$$\underline{B}_s \leq b_s(t-1) \leq \overline{B}_s, \tag{7b}$$

where $\underline{R}_s < 0$ and $\overline{R}_s > 0$ are the ramp rate limits, and $\underline{B}_s < \overline{B}_s$ are fixed bounds. Although in principle a battery could be completely discharged, it is advisable to avoid full discharge in order to prolong battery life. To this aim, let the depth of discharge (DOD) of the storage at bus s and time t be defined as $D_s(t) = 1 - e_s(t)/E_s$. For a fixed critical DOD value $\overline{D}_s < 1$ at bus s, we consider the soft constraint

$$D_s(t) \leq \overline{D}_s + \delta_s(t), \tag{8}$$

where the slack variable $\delta_s(t)$, satisfying

$$\delta_s(t) \geq 0, \tag{9}$$

enables to exceed the critical DOD value at bus s and time t, if needed. In this way, full discharge can be limited by minimizing some specific function of $\delta_s(t)$.

For a generic bus $k \in \mathcal{N}^L$ having loads, generators and ESSs connected to it, $P_k(t)$ and $Q_k(t)$ in (2) can be decomposed as

$$P_k(t) = P_k^G(t) - P_k^D(t) - r_k(t-1) \tag{10a}$$

$$Q_k(t) = Q_k^G(t) - Q_k^D(t) - b_k(t-1), \tag{10b}$$

where the superscript ^{G} refers to generation and the superscript ^{D} refers to demand. The following additional constraints apply to buses not equipped with ESSs:

$$r_h(t-1) = b_h(t-1) = 0, \quad h \in \mathcal{N}^L \backslash \mathcal{S}. \tag{11}$$

The quantities $P_k^D(t)$, $Q_k^D(t)$, $P_k^G(t)$ and $Q_k^G(t)$ are considered as known inputs in (10). In case no load or generator is connected to bus k, the corresponding demand or generation are assumed to be zero.

B. Optimal ESS operation

In the following problem formulation, we provisionally assume that future demand and generation, i.e. the quantities $P_k^D(t)$, $Q_k^D(t)$, $P_k^G(t)$ and $Q_k^G(t)$, are known. We will remove this assumption in the next section.

To define a suitable cost function to be optimized, we recall that the major amount of losses in a power system (estimated around 70% of the total) is in distribution lines. This suggests that minimizing line losses should be a primary objective in the operation of distribution networks. Moreover, battery degradation, depending on both usage and DOD, is another issue to take into account. Hence, the following instantaneous cost incurred at time t is introduced:

$$C(t) = C_L(t) + \gamma_U C_U(t) + \gamma_D C_D(t), \tag{12}$$

where $\gamma_U, \gamma_D, \geq 0$ are suitable weights, and

- $C_L(t)$ represents the total real losses in the network,

$$C_L(t) = \sum_{k \in \mathcal{N}} P_k(t) \Delta T, \tag{13}$$

- $C_U(t)$ is a measure of the battery usage,

$$C_U(t) = \sum_{s \in \mathcal{S}} |r_s(t-1)| \Delta T, \tag{14}$$

- $C_D(t)$ quantifies the violations of the critical DOD values,

$$C_D(t) = \sum_{s \in \mathcal{S}} \delta_s(t). \tag{15}$$

At time t_0 and for a fixed control horizon H, the considered control problem aims at finding an ESS operating policy such that the sum of $C(t)$ in (12) over $\mathcal{T} = \{t_0+1, \ldots, t_0+H\}$ is minimized, while satisfying the voltage magnitude and real power flow constraints. This translates into the following multi-period OPF problem, where the free variables are represented by $V_k(t)$, $r_s(t-1)$, $b_s(t-1)$ and $\delta_s(t)$ for all $k \in \mathcal{N}^L$, $s \in \mathcal{S}$ and $t \in \mathcal{T}$:

$$\min_{V_k(t), r_s(t-1), b_s(t-1), \delta_s(t)} \sum\nolimits_{t \in \mathcal{T}} C(t) \tag{16}$$
$$\text{s. t.} \quad (2)-(11), \quad k \in \mathcal{N}^L,\ s \in \mathcal{S},\ (i,j) \in \mathcal{E},\ t \in \mathcal{T}.$$

In the following, the values of the control variables $r_k(t_0)$ and $b_k(t_0)$ at the optimum of problem (16) will be denoted by $r_k^*(t_0)$ and $b_k^*(t_0)$.

Since problem (16) is non-convex, and therefore difficult to solve, a common approach adopted in the literature is to compute an approximated solution through convex relaxations based on semidefinite programming (SDP), see, e.g., [10], [11]. In general, the relaxation provides a lower bound to the optimal cost of (16), but it is shown empirically in [12] that it works particularly well for networks with radial layout, which are frequent in LV public distribution systems of many countries worldwide. Necessary conditions under which the relaxation is exact, are provided in [13].

III. Receding horizon implementation

The practical implementation of problem (16) struggles with the fact that future demand and generation are unknown at time t_0. For this reason, the values $P_k^D(t_0+h)$, $Q_k^D(t_0+h)$, $P_k^G(t_0+h)$ and $Q_k^G(t_0+h)$, are replaced in practice with their forecasts computed at time t_0, namely the values $\hat{P}_k^D(t_0+h|t_0)$, $\hat{Q}_k^D(t_0+h|t_0)$, $\hat{P}_k^G(t_0+h|t_0)$ and $\hat{Q}_k^G(t_0+h|t_0)$, $h = 1, \ldots, H$.

Regarding the choice of the control horizon H in problem (16), on the one hand, the larger the control horizon H, the more efficient the ESS operating policy in terms of line losses and operation costs. On the other hand, prediction accuracy typically gets worse for large lead times, and therefore the ESS operating policy obtained by solving problem (16) under predicted demand and generation will likely not be optimal under the true realization of these quantities. More importantly, it could also fail in satisfying the voltage magnitude and real power flow constraints. This implies that a suitable trade-off should be found when selecting H in real applications. Values ranging from two to three hours are deemed to be a realistic compromise for LV networks under consideration.

One way to mitigate the effects of uncertainties such as inaccurate forecasts, is to apply the receding horizon approach which is typical of model predictive control [14]. The idea is that problem (16) is solved at time t_0 based on available demand and generation forecasts. Then, only the values $r_s^*(t_0)$ and $b_s^*(t_0)$ are applied. The same steps are repeated at the next time instants by exploiting the updated demand and generation forecasts that become available. The complete receding horizon procedure is reported in Algorithm 1.

Algorithm 1 Receding horizon procedure for ESS operation

for $t_0 = 0, 1, \ldots$ **do**
  Acquire the current battery state $e_s(t_0)$ for all $s \in \mathcal{S}$
  Compute forecasts $\hat{P}_k^D(t_0+h|t_0)$, $\hat{Q}_k^D(t_0+h|t_0)$, $\hat{P}_k^G(t_0+h|t_0)$ and $\hat{Q}_k^G(t_0+h|t_0)$ for all $k \in \mathcal{N}^L$ and $h = 1, \ldots, H$
  Solve problem (16)
  Apply control values $r_k^*(t_0)$ and $b_k^*(t_0)$
end for

IV. Load and generation forecasting

The performance of the receding horizon approach for ESS operation described in Section III depends, among other factors, on the accuracy of demand and generation forecasts. In order to reliably predict these quantities at each bus of the network, measurements would be needed in real-time. Unfortunately, the high cost of measurement and communication infrastructures makes them unavailable in most LV networks worldwide. Even when smart meters are installed, recorded measurements are typically transferred to data collectors in a batch way, e.g. monthly. Therefore, these measurements can be used for estimating the models of demand and generation, but cannot be assumed to be available in real-time for network operation.

In this paper, we consider a measurement setting which is deemed to be as realistic as possible. We assume that a historical data set of load and generation at all the buses of the LV network is available (e.g., from smart meters). This data set is used to estimate (and update, as soon as new data become available) the models of demand and generation in the network. The requirement for real-time measurements is limited to the active power P_1 injected at the slack bus and the meteorological variables useful to predict generation from renewable energy sources. For instance, measurements of solar irradiance I and outdoor temperature T are required in case PV generation is present. To reduce the requirements for the communication infrastructure, meteorological variables are measured at the MV/LV substation, where the control logic is installed. This assumption is also practically motivated by the fact that LV networks typically do not cover large areas, and are therefore characterized by a limited variability of meteorological variables.

In the following, the average active power P_1 injected at the slack bus between $t-1$ and t is decomposed in the form

$$P_1(t) = P^A(t) - P^G(t) + P^S(t), \tag{17}$$

where $P^G(t) = \sum_{k\in\mathcal{N}^L} P_k^G(t)$ is the aggregate generation of the network, $P^S(t) = \sum_{s\in\mathcal{S}} r_s(t-1)$ is the total active power exchanged by the ESSs, and $P^A(t) = \sum_{k\in\mathcal{N}^L} P_k^D(t) + P^L(t)$ is the aggregate demand of the network, including the losses $P^L(t)$ as a fictitious load. The focus will be on how to predict P^A and P^G, and infer from these predictions the forecasts of P_k^D and P_k^G for all $k \in \mathcal{N}^L$. Then, the forecasts of Q_k^D and Q_k^G are obtained by applying a fixed power factor, which is typically between 0.9 and 1 for loads, and almost 1 for PV generators connected to the network through grid-tie inverters.

A. PV generation forecasting

In this paper, for the sake of simplicity, we assume that generation in the LV network is only of PV type, as is often the case. Therefore, P^G in (17) can be seen as the aggregate PV generation in the network, which can be described as a function of the solar irradiance I and the outdoor temperature T through the PVUSA model

$$P^G(t) = a\, I(t) + b\, I^2(t) + c\, I(t)T(t), \tag{18}$$

where $a > 0$, $b < 0$ and $c < 0$ are the model parameters [15]. The PVUSA model is linear-in-the-parameters, and therefore parameter estimation can be performed very efficiently via least squares [16]. Here we assume that a, b and c were estimated from the available historical data set of generation, solar irradiance and outdoor temperature.

Given (18), a strategy for predicting P^G consists in using the forecasts of I and T in the equation of the PVUSA model. Forecasting models of solar irradiance, mainly based on time series analysis and artificial neural networks, can be found in the literature, see, e.g., [17], [18]. Modeling and prediction of outdoor temperature can be addressed through the use of seasonal time series models, see [19]. Then, the forecast of P^G can be split among buses with generation proportionally to the power installed at each bus.

B. Load forecasting

Load demand exhibits strong seasonal behavior on different time scales. In our setting, this applies to the aggregate demand P^A in (17), and therefore seasonal time series models can be adopted for modeling and prediction of P^A, see [19], [20]. One practical issue to be considered here is that measurements of P^A are not available in real-time, and hence pseudo-measurements $\widetilde{P}^A$ should be used in place of P^A. These can be defined from (17) as

$$\widetilde{P}^A(t) = P_1(t) + \widetilde{P}^G(t) - P^S(t), \tag{19}$$

where $\widetilde{P}^G$ is the pseudo-measurement of P^G computed by substituting the measured values of I and T into (18). Note that, in (19), both P_1 and P^S are known: the former is measured, while the latter is decided by the ESS control policy at time $t-1$ (see Section III).

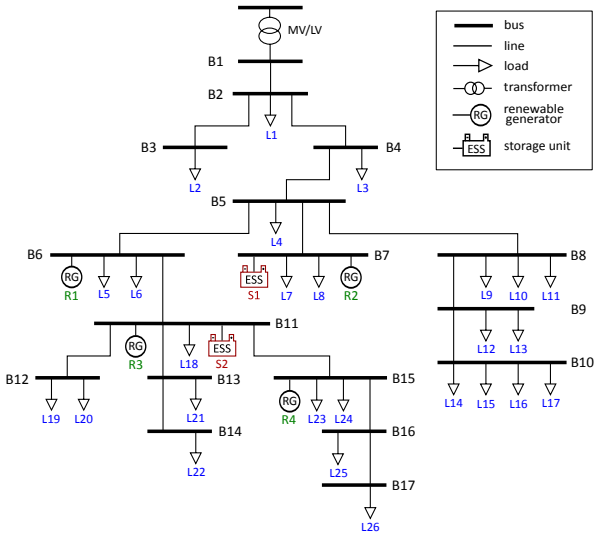

Fig. 1. Italian LV test network.

Once a forecast of P^A is available, the problem is how to use this value to infer the load at each bus $k \in \mathcal{N}^L$. To this aim, we introduce $\omega_k(\tau)$ as the average fraction of the aggregate demand at bus k and time τ of the day, $\tau = 0, 1, \ldots, N_d - 1$, where N_d is the number of samples per day. The value of $\omega_k(\tau)$ is computed on an estimation data set as

$$\omega_k(\tau) = \frac{1}{L}\sum_{\ell=0}^{L-1} \frac{P_k^D(\tau + \ell\, N_d)}{P^A(\tau + \ell\, N_d)}, \tag{20}$$

where L is the number of days in the data set. Given the forecast aggregate demand $\hat{P}^A(t+h|t)$, the prediction $\hat{P}_k^D(t+h|t)$ of the load at bus $k \in \mathcal{N}^L$ is obtained as

$$\hat{P}_k^D(t+h|t) = \omega_k\big((t+h) \bmod N_d\big)\hat{P}^A(t+h|t), \tag{21}$$

where mod is the modulo operation. This is, for instance, the method actually used by the main Italian DSO for monitoring LV networks. In practice, it is also possible to make the fraction $\omega_k(\tau)$ depend on the day of the week in order to take into account different patterns of the aggregate demand, e.g., in weekdays and weekends. Notice that $\sum_{k\in\mathcal{N}^L} \omega_k(\tau)$ does not sum up to 1, in general, due to the fraction of active power dissipated in the lines.

V. Numerical results

The proposed ESS control algorithm has been tested on real data from a real LV network, whose topology was provided by the main Italian DSO. The test network, shown in Fig. 1, consists of $n = 17$ buses, hosting 26 loads and 4 PV units. For all buses $k \in \mathcal{N}^L$, in accordance with the European Norm 50160, a 10% tolerance around the nominal voltage value is allowed in both directions, i.e. $\underline{v}_k = 0.9$ pu and $\overline{v}_k = 1.1$ pu in (3). Bounds $\overline{P}_{ij}$ on the real power flow in (4) are all set to 20 kW. For all loads and generators, three months of active and reactive power profiles are available with time step of 15 minutes, therefore we assume $\Delta T = 900$ s and $N_d = 96$. Measurements of

solar irradiance and outdoor temperature are also available with the same resolution.

Two ESSs are assumed to be installed in the network. ESS locations and sizes are decided according to the procedure described in [6]. In particular, the ESSs are placed at buses 7 and 11, with capacities equal to $E_7 = 15$ kWh and $E_{11} = 55$ kWh, respectively. Active ramp limits in (7a) are chosen such that $\overline{R}_s = -\underline{R}_s = 15$ kW, and the bounds $\underline{B}_s$ and $\overline{B}_s$ in (7b) are set to keep the phase angle shift between -10 and +10 deg. Moreover, ESS levels lower then 30% of their nominal capacity are penalized, i.e. $\overline{D}_7 = \overline{D}_{11} = 0.7$ in (8).

The weights in the total cost (12) are set to $\gamma_U = 0.1$ and $\gamma_D = 0.25$ kWh, whereas the control horizon of problem (16) is chosen to be $H = 8$ samples, corresponding to 2 hours.

A. Performance of ESS control

First, the historical data sets of load and generation are used to estimate the load fractions $\omega_k(\tau)$ in (21) and the parameters of the PVUSA model (18), as well as of the time series models of aggregate load, solar irradiance and outdoor temperature, as described in Section IV.

Second, the control algorithm described in Section III is tested on two challenging days featuring overvoltages (day-1) and undervoltages (day-2) when no voltage control is applied. At each time step $t = 0, 1, 2, \ldots, N_d - 1$, demand and generation in the network are predicted for lead times h ranging from one sample (15 min ahead) to eight samples (2 hours ahead). Figure 2 shows an example of aggregate demand (top), solar irradiance (middle) and outdoor temperature (bottom) forecasts. Then, an SDP relaxation of problem (16) is solved using the SeDuMi solver [21]. The actual effect of the control inputs $r_s^*(t)$ and $b_s^*(t)$ is simulated through a load flow at time $t+1$ under the true demand and generation.

In order to evaluate the benefits of using the ESSs to tackle voltage problems, we define the total voltage violation at bus k over the considered time horizon as

$$\nu_k = \frac{1}{N_d} \sum_{t=0}^{N_d-1} [\underline{v}_k - |V_k(t)|]^+ + [|V_k(t)| - \overline{v}_k]^+, \qquad (22)$$

where $[x]^+ = \max(x, 0)$. Let ν_k^N be (22) evaluated in the case without ESSs, and ν_k^C in the case with ESSs. We then define the performance index

$$\eta = \left(1 - \frac{\sum_{k \in \mathcal{N}^L} \nu_k^C}{\sum_{k \in \mathcal{N}^L} \nu_k^N}\right) \cdot 100\%. \qquad (23)$$

Assuming that the denominator of (23) is greater than zero (i.e., at least one violation of the voltage bounds occurs anywhere in the network over the considered time horizon), η quantifies how much the ESSs succeed in preventing the voltage problems. It turns out that $\eta = 100\%$ for day-1, i.e. all voltages are kept within the bounds thanks to the use of ESSs, whereas $\eta = 98.2\%$ for day-2, meaning that voltage violations are almost completely avoided or mitigated. This can be observed in Fig. 3 (top), showing the plots of voltage magnitudes at all the buses of the network in the cases with and without ESSs. From Fig. 3 (bottom), it can be also observed that the ESS control manages to counteract voltage problems while also reducing total line losses of more than 40% in both days. In particular, most of the reduction is achieved during peak hours of PV generation.

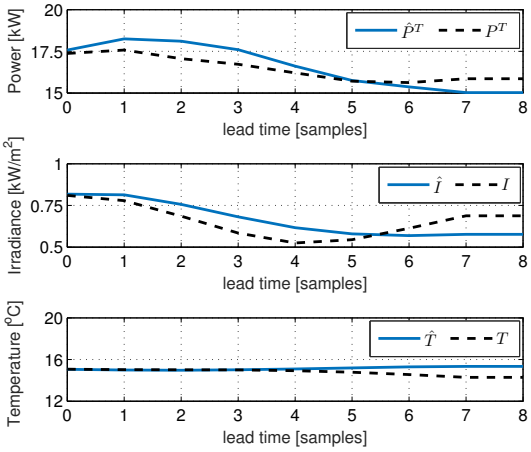

Fig. 2. Examples of forecasts of aggregate demand (top), solar irradiance (middle) and outdoor temperature (bottom) at time 12:00AM of day-1 with prediction horizon of $H = 8$ samples (2 hours): actual (black dashed lines) and predicted profiles (blue solid lines).

Finally, Fig. 4 shows the plots of storage levels and active power injected into the ESSs for both test days. It can be noticed that the optimal control policy obtains to operate the ESSs as little as possible. Indeed, the active power injected into the ESSs is kept equal to zero for most of the time, thus contributing to prolong battery life.

VI. Conclusions

This paper addressed the problem of controlling ESSs in an LV electricity grid for preventing over- and undervoltages. The proposed control algorithm borrows ideas from the classical receding horizon control approach. At each time step a multi-period OPF problem is solved with the objective of minimizing line losses and storage usage, while maintaining the voltage magnitude at all buses within the specified limits. Only the power exchanged with the MV network and some meteorological variables are monitored in order to predict the future state of the network and any potential voltage rise/drop. The application to a data set from a real Italian LV network shows the potential of the proposed approach to enhance the voltage quality at customers' premises.

References

[1] A. T. Procopiou, C. Long, and L. F. Ochoa, "Voltage control in LV networks: An initial investigation," in *Proc. 5th IEEE/PES Innov. Smart Grid Technol. Europe*, Istanbul, Turkey, 2014.

[2] J. Tuominen, S. Repo, and A. Kulmala, "Comparison of the low voltage distribution network voltage control schemes," in *Proc. 5th IEEE/PES Innov. Smart Grid Technol. Europe*, Istanbul, Turkey, 2014.

[3] L. Wang, D. H. Liang, A. F. Crossland, P. C. Taylor, D. Jones, and N. S. Wade, "Coordination of multiple energy storage units in a low-voltage distribution network," *IEEE Trans. Smart Grid*, vol. 6, no. 6, pp. 2906–2918, 2015.

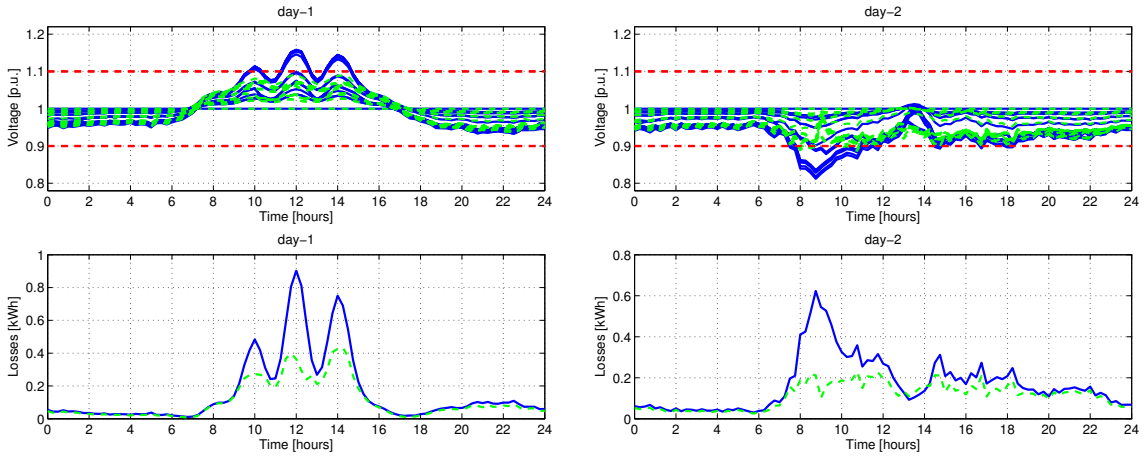

Fig. 3. Performance of the receding horizon control algorithm on day-1 (left) and day-2 (right). Top: Voltage magnitudes at all buses $k \in \mathcal{N}^L$ with ESSs (green dashed lines) and without ESSs (blue solid lines). Bottom: Line losses with ESSs (green dashed line) and without ESSs (blue solid line).

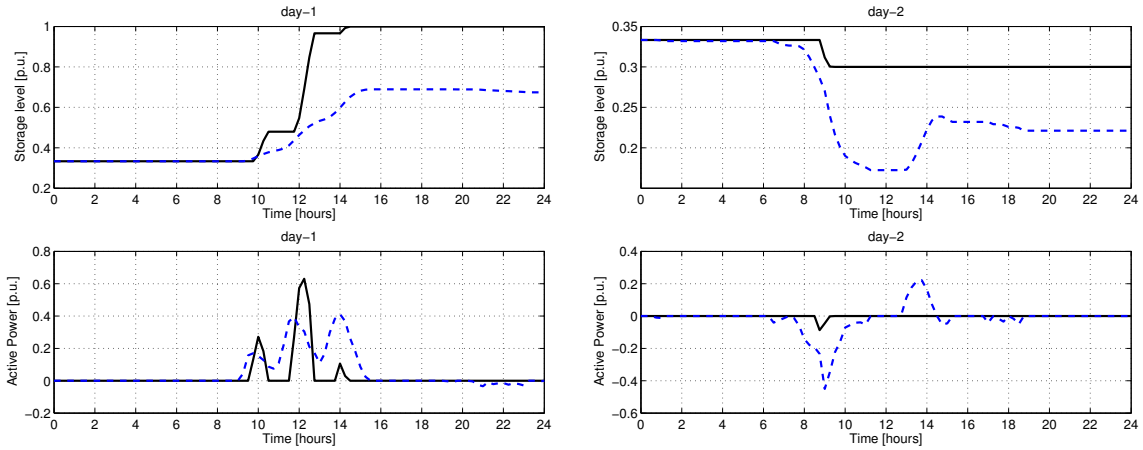

Fig. 4. Operation of ESS 7 (black solid line) and ESS 11 (blue dashed line) during day-1 (left) and day-2 (right). Top: ESS levels. Bottom: ESS active power controls.

[4] H. Nazaripouya, Y. Wang, P. Chu, H. R. Pota, and R. Gadh, "Optimal sizing and placement of battery energy storage in distribution system based on solar size for voltage regulation," in *Proc. IEEE Power Energy Soc. Gen. Meeting*, Denver, CO, USA, 2015.

[5] M. Nick, R. Cherkaoui, and M. Paolone, "Optimal siting and sizing of distributed energy storage systems via alternating direction method of multipliers," *Int. J. Elect. Power Energy Syst.*, vol. 72, pp. 33–39, 2015.

[6] A. Giannitrapani, S. Paoletti, A. Vicino, and D. Zarrilli, "Optimal allocation of energy storage systems for voltage control in LV distribution networks," *IEEE Trans. Smart Grid*, vol. PP, no. 99, pp. 1–12, 2016.

[7] A. T. Procopiou, C. Long, and L. F. Ochoa, "On the effects of monitoring and control settings on voltage control in PV-rich LV networks," in *Proc. IEEE Power Energy Soc. Gen. Meeting*, Denver, CO, USA, 2015.

[8] P. Malysz, S. Sirouspour, and A. Emadi, "An optimal energy storage control strategy for grid-connected microgrids," *IEEE Trans. Smart Grid*, vol. 5, no. 4, pp. 1785–1796, 2014.

[9] A. Parisio, E. Rikos, and L. Glielmo, "A model predictive control approach to microgrid operation optimization," *IEEE Trans. Control Syst. Technol.*, vol. 22, no. 5, pp. 1813–1827, 2014.

[10] S. Low, "Convex relaxation of optimal power flow – Part I: Formulations and equivalence," *IEEE Trans. Control Netw. Syst.*, vol. 1, no. 1, pp. 15–27, 2014.

[11] D. Gayme and U. Topcu, "Optimal power flow with large-scale storage integration," *IEEE Trans. Power Syst.*, vol. 28, no. 2, pp. 709–717, 2013.

[12] L. Gan and S. H. Low, "Convex relaxations and linear approximation for optimal power flow in multiphase radial networks," in *Proc. 18th Power Syst. Comp. Conf.*, Wroclaw, Poland, 2014.

[13] S. H. Low, "Convex relaxation of optimal power flow – Part II: Exactness," *IEEE Trans. Control Netw. Syst*, vol. 1, no. 2, pp. 177–189, 2014.

[14] J. M. Maciejowski, *Predictive control with constraints*. Pearson Education, 2002.

[15] R. N. Dows and E. J. Gough, "PVUSA procurement, acceptance, and rating practices for photovoltaic power plants," Pacific Gas and Electric Company, San Ramon, CA, Tech. Rep., 1995.

[16] G. Bianchini, S. Paoletti, A. Vicino, F. Corti, and F. Nebiacolombo, "Model estimation of photovoltaic power generation using partial information," in *Proc. 4th IEEE/PES Innov. Smart Grid Technol. Europe*, Copenhagen, Denmark, 2013.

[17] J. Wu and C. K. Chan, "Prediction of hourly solar radiation using a novel hybrid model of ARMA and TDNN," *Solar Energy*, vol. 85, no. 5, pp. 808–817, 2011.

[18] G. Reikard, "Predicting solar radiation at high resolutions: A comparison of time series forecasts," *Solar Energy*, vol. 83, no. 3, pp. 342–349, 2009.

[19] G. E. P. Box, G. M. Jenkins, and G. C. Reinsel, *Time Series Analysis: Forecasting and Control*, 4th ed. Wiley, 2008.

[20] A. Garulli, S. Paoletti, and A. Vicino, "Models and techniques for electric load forecasting in the presence of demand response," *IEEE Trans. Control Syst. Technol.*, vol. 23, no. 3, pp. 1087–1097, 2015.

[21] J. Sturm, "Using SeDuMi 1.02, A Matlab toolbox for optimization over symmetric cones," *Optim. Methods Softw.*, vol. 11, no. 1-4, pp. 625–653, 1999.